Synchronization of electrically coupled stochastic magnetic oscillators induced by thermal and electrical noise

A. Mizrahi,[1,2] N. Locatelli,[2] J. Grollier,[1] and D. Querlioz[2]
[1]*Unite Mixte de Physique CNRS/Thales, Universite Paris-Sud, Universite Paris-Saclay, 91767 Palaiseau, France*
[2]*Institut dElectronique Fondamentale, Universite Paris-Sud, CNRS, Universite Paris-Saclay, 91405 Orsay, France*
(Received 29 June 2016; published 17 August 2016)

Superparamagnetic tunnel junctions are nanostructures that auto-oscillate stochastically under the effect of thermal noise. Recent works showed that despite their stochasticity, such junctions possess a capability to synchronize to subthreshold voltage drives, in a way that can be enhanced or controlled by adding noise. In this work, we investigate a system composed of two electrically coupled junctions, connected in series to a periodic voltage source. We make use of numerical simulations and of an analytical model to demonstrate that both junctions can be phase locked to the drive, in phase or in antiphase. This synchronization phenomenon can be controlled by both thermal and electrical noises, although the two types of noises induce qualitatively different behaviors. Namely, thermal noise can stabilize a regime where one junction is phase locked to the drive voltage while the other is blocked in one state; on the contrary, electrical noise causes the junctions to have highly correlated behaviors and thus cannot induce the latter. These results open the way for the design of superparamagnetic tunnel junctions that can perform computation through synchronization, and which harvest the largest part of their energy consumption from thermal noise.

DOI: 10.1103/PhysRevB.94.054419

I. INTRODUCTION

Superparamagnetic tunnel junctions are stochastic auto-oscillators, powered by thermal noise [1]. They naturally transform the fluctuations of thermal noise into a large telegraphic signal that can be read through a simple measurement of their electrical resistance. Furthermore, they have the ability to exhibit the phenomenon of stochastic resonance in which noise enables a weak signal to be detected by a nonlinear system [2–4]. In previous works, we showed how they can also synchronize to a weak periodic voltage through both thermal noise and electrical noise on the drive [5,6]. The capacity of superparamagnetic tunnel junctions to harvest the energy of noise provides the opportunity to study their physics under many angles, from sensing to low-power computing. This requires understanding how these noise-induced phenomena occur in systems composed of several coupled superparamagnetic tunnel junctions. Noise-induced synchronization of coupled elements has been studied for several systems, such as arrays of generic nonlinear elements [7–9] or linear chains of diffusely coupled diode resonators [10], but their analysis does not apply to our specific device as they consider linear coupling and collective phenomena. Furthermore, these works focus on noise-induced signal power amplification but do not study frequency locking and phase locking directly.

In this work, we present a theoretical study of noise-induced synchronization of two electrically coupled superparamagnetic tunnel junctions. Our comprehensive study is based on numerical simulations. We examine frequency locking through the evolution with noise of the junctions' frequencies as well as phase locking through time-resolved traces of the junctions' resistances. All results are discussed with the support of an analytical model based on the evolution with noise of the junctions' switching probabilities. Both numerical and analytical models were previously validated by direct comparison to experiments in the case of the synchronization of a single junction [6,11]. We examine the differences between the synchronization phenomena induced by thermal noise versus those induced by electrical noise on the drive voltage.

After presenting our model in the case of a single superparamagnetic tunnel junction, we apply it to two junctions connected in series to a periodic voltage source. We show that both junctions can be synchronized simultaneously to the voltage drive. Both in-phase-locking and antiphase-locking configurations can be achieved by choosing the connections of the junctions in the circuit. These phenomena can be induced and controlled by the amplitudes of thermal and electrical noises. Specifically, we show that thermal noise is able to stabilize a hybrid synchronization regime where, at each oscillation of the drive, one randomly chosen junction is phase locked to the drive while the other is blocked in one state. On the other hand, this regime cannot be achieved by the addition of electrical noise. The electrical noises on the two junctions both come from the drive and are thus correlated. The switches of the junctions are simultaneous and triggered by large voltage events.

II. NOISE-INDUCED SYNCHRONIZATION OF A SINGLE JUNCTION

A magnetic tunnel junction is composed of two ferromagnets (one with pinned magnetization and one with free magnetization) and a tunnel barrier sandwiched between them [Fig. 1(a)]. The magnetization of the free layer has two stable states: parallel (P) and antiparallel (AP) to the magnetization of the pinned layer. The antiparallel state has a higher electrical resistance than the parallel state. Magnetic tunnel junctions can be engineered so that the energy barrier between the P and AP states is low enough to reach the superparamagnetic regime. This means that the intrinsic thermal noise in the junction induces random, spontaneous switches of the magnetization between the P and AP states. The superparamagnetic tunnel

 ©2016 American Physical Society

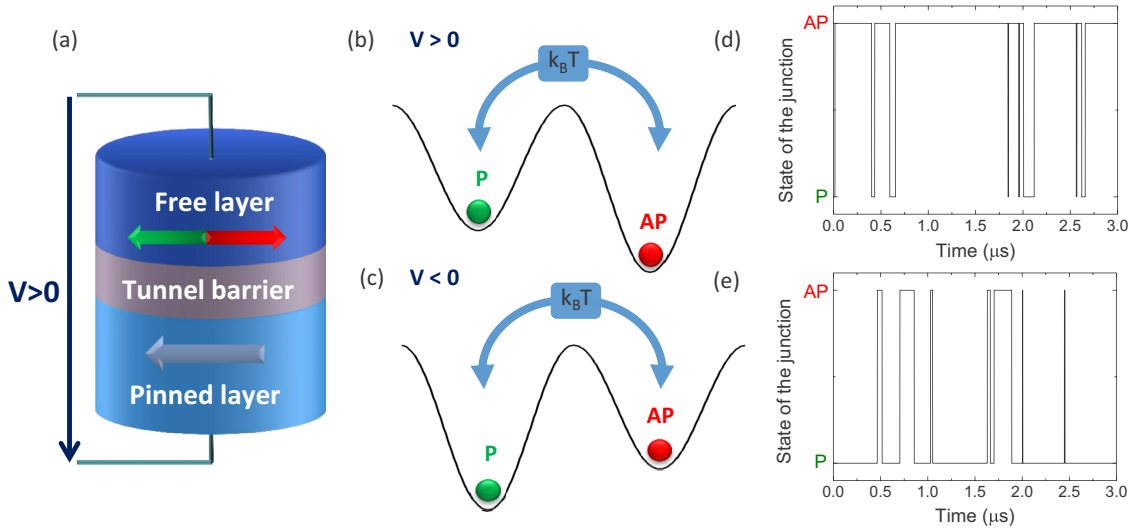

FIG. 1. (a) Schematic view of a magnetic tunnel junction. (b),(c) Energy landscape of the system when a (b) positive or (c) negative voltage is applied. (d),(e) Numerical simulations of the state of a junction vs time for applied voltages of $V = +0.17V_c$ and $V = -0.17V_c$, at a temperature $T = 300$ K.

junction behaves as a noise-powered stochastic oscillator [1,5], as depicted in Figs. 1(d) and 1(e), which does not need any external supply of energy to run. The phenomenon of spin-transfer torque [12,13] provides a handle over the junction as a positive voltage stabilizes the AP state [Figs. 1(b) and 1(d)], while a negative voltage stabilizes the P state [Figs. 1(c) and 1(e)]. The applied dc voltage is defined as positive from the pinned layer to the free layer. Thermal energy destabilizes both states.

A. Methods

Making the assumption that the free layer of the junction can be considered as a single-domain magnetization element, the probabilities to leave the AP and P states within a duration t can be described by a Poisson process:

$$P_{\mathrm{AP}\to P}(V,t) = 1 - \exp[-\phi_{\mathrm{AP}}(V)t], \tag{1}$$

$$P_{P\to \mathrm{AP}}(V,t) = 1 - \exp[-\phi_{P}(V)t]. \tag{2}$$

The escape rates $\phi_{\mathrm{AP}(P)}$ are described by the Neel-Brown model [14] and follow the Arrhenius equations. They can be tuned by the voltage applied to the junction, through the effect of spin-transfer torque [15,16]:

$$\phi_{\mathrm{AP}}(V) = \phi_0 \exp\left[-\frac{\Delta E}{k_B T}\left(1 + \frac{V}{V_c}\right)\right], \tag{3}$$

$$\phi_{P}(V) = \phi_0 \exp\left[-\frac{\Delta E}{k_B T}\left(1 - \frac{V}{V_c}\right)\right], \tag{4}$$

where $\phi_0 = 10^9$ Hz is the effective attempt rate [1], ΔE is the energy barrier between the two stable states, k_B is the Boltzmann constant, T is the temperature, V is the voltage across the junctions, and V_c is the threshold voltage for deterministic switching at 0 K [16].

Below, we consider junctions with an energy barrier and temperature such that $\Delta E = 30\,k_B T$ at $T = 50$ K and a threshold voltage $V_c = 1$ V. First, a junction is submitted to a square periodic voltage with frequency $F_{ac} = 1/T_{ac} = 1$ MHz and with subthreshold amplitude $V = 0.75$ V.

We perform numerical simulations of the system as follows. At each time step of $dt = 10$ ns, the probability for the junction to switch from one state to the other is computed through Eqs. (1)–(4). A uniform pseudorandom number between 0 and 1 is generated. If the random number is lower than the switching probability, the junction changes state. In the considered range of noise, events shorter than dt are rare enough to be nonsignificant.

B. Thermal-noise-induced synchronization

Synchronization of the junction to the weak periodic signal can be controlled by different sources of noise. We first study the influence of thermal noise.

Figure 2(a) represents the frequency of the junction—defined as the mean number of oscillations of the junction's state per second—versus temperature. The frequency increases with temperature and presents a plateau at the frequency of the drive F_{ac}. This plateau is a signature of stochastic resonance and noise-induced synchronization [17,18].

The junction is considered to be in phase with the drive if it is in the AP state when the drive is $+V$ and in the P state when the drive is $-V$. Consequently, we can define P_+ as the probability to phase lock to the drive and P_- as the probability to phase unlock:

$$P_+ = P_{P\to\mathrm{AP}}\left(+V, \frac{T_{ac}}{2}\right) = P_{\mathrm{AP}\to P}\left(-V, \frac{T_{ac}}{2}\right) = 1 - \exp\left(-\frac{T_{ac}}{2}\phi_+\right), \tag{5}$$

$$P_- = P_{P\to\mathrm{AP}}\left(-V, \frac{T_{ac}}{2}\right) = P_{\mathrm{AP}\to P}\left(+V, \frac{T_{ac}}{2}\right) = 1 - \exp\left(-\frac{T_{ac}}{2}\phi_-\right), \tag{6}$$

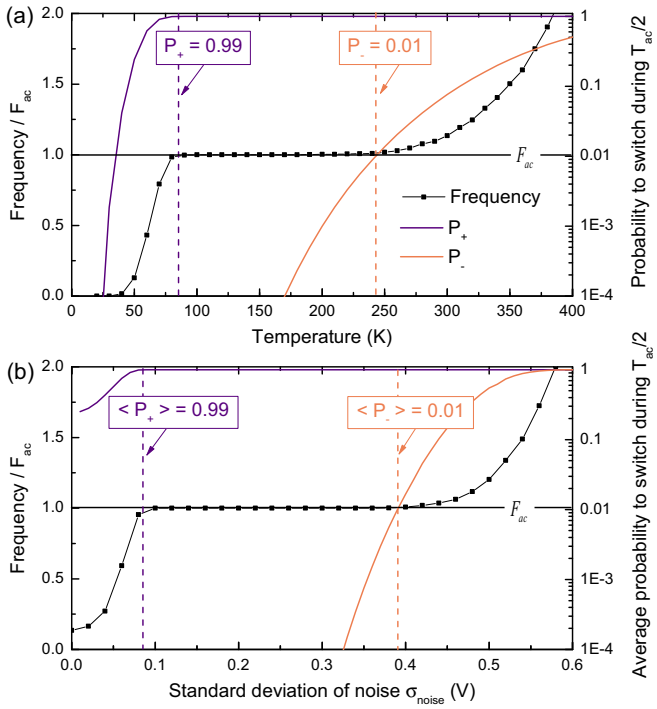

FIG. 2. (a) The frequency of the stochastic oscillator is plotted vs temperature in blue squares (in units of the drive frequency F_{ac}). The probabilities to phase lock P_+ and unlock P_- are plotted vs temperature in purple and orange solid lines, respectively. The drive frequency F_{ac} is represented by a black horizontal line. The temperatures for which $P_+ = 0.99$ and $P_- = 0.01$ are represented by purple and orange vertical dashed lines, respectively. (b) The frequency of the stochastic oscillator, as well as the average probabilities to phase lock and unlock, are plotted vs the standard deviation of the white Gaussian electrical-noise distribution. The same legend is used for both (a) and (b).

where

$$\phi_+ = \phi_0 \exp\left[-\frac{\Delta E}{k_B T}\left(1 - \frac{V}{V_c}\right)\right], \tag{7}$$

$$\phi_- = \phi_0 \exp\left[-\frac{\Delta E}{k_B T}\left(1 + \frac{V}{V_c}\right)\right]. \tag{8}$$

For each temperature, the probabilities P_+ and P_- are computed analytically and plotted in Fig. 2(a).

At low temperatures (below 85 K), the frequency of the junction is lower than the drive frequency F_{ac}. Indeed the drive is too weak to induce synchronization by itself because its amplitude is subthreshold ($V = 0.75V_c$).

We investigate the conditions leading to the occurrence of synchronization. When the junction and the drive are out of phase, they have a probability P_+ to phase lock in the next half period $\frac{T_{ac}}{2}$ (before the next switch of the drive). When the junction and the drive are in phase, they have a probability $1 - P_-$ to stay phase locked during the next half period. As the junction is intrinsically stochastic, there cannot be perfect deterministic synchronization.

We consider the junction to be synchronized to the drive for $P_+ > 0.99$ and $P_- < 0.01$. This corresponds to the temperature range $85 < T < 241$ K and indeed we observe that it matches the visual boundaries of the plateau where the frequency of the junction is equal to the frequency of the drive. Modifying the characteristics of the junction modifies the boundaries of the synchronization range: choosing, for instance, a barrier of $\Delta E/k_B T = 40$ at $T = 50$ K allows for synchronization at room temperature [5].

Above $T = 241$ K, the probability to phase unlock P_- is higher than 0.01. We observe that the junction regularly slips out of phase. These parasitic oscillations—here called glitches—raise the frequency of the junction above F_{ac} and destroy synchronization.

C. Electrical-noise-induced synchronization

Synchronization can also be induced by electrical noise added to the drive signal. We apply a voltage $U(t) = V_{ac}(t) + N(t)$ to the junction. $V_{ac}(t)$ is a square periodic drive of frequency $F_{ac} = 1$ MHz and amplitude $V = 0.75$ V. $N(t)$ is a white Gaussian noise with standard deviation σ_{noise} and cutoff frequency $F_{\text{noise}} = 100$ MHz. The escape rates ϕ_+ and ϕ_- are time-dependent random variables:

$$\phi_+(t) = \phi_0 \exp\left\{-\frac{\Delta E}{k_B T}\left[1 - \frac{V + N(t)}{V_c}\right]\right\}, \tag{9}$$

$$\phi_-(t) = \phi_0 \exp\left\{-\frac{\Delta E}{k_B T}\left[1 + \frac{V + N(t)}{V_c}\right]\right\}. \tag{10}$$

In this case, the switching probabilities need to be averaged over all possible values of N. The average probabilities to phase lock and unlock can be computed as follows:

$$\langle P_\pm \rangle = 1 - \left[\int_{-\infty}^{+\infty}\left(1 - \exp\left\{-\delta t \phi_0 \exp \times \left[-\frac{\Delta E}{kT}\left(1 \pm \frac{V + N}{Vc}\right)\right]\right\}\right)\psi(N)dN\right]^{\frac{T_{ac}}{2\delta t}}, \tag{11}$$

where $\delta t = 1/F_{\text{noise}}$ is the smallest time scale of the electrical noise and $\psi(N)$ is a Gaussian distribution with standard deviation σ_{noise}.

In Fig. 2(b), the frequency of the junction obtained by numerical simulations as well as the average probabilities $\langle P_+ \rangle$ and $\langle P_- \rangle$ are plotted versus the noise's standard deviation σ_{noise}. The frequency exhibits again a plateau at F_{ac}. Noise-induced synchronization with the drive V_{ac} is achieved for an optimal range of electrical noise $0.08 < \sigma_{\text{noise}} < 0.39$ V, which corresponds to $\langle P_+ \rangle > 0.99$ and $\langle P_- \rangle < 0.01$.

In conclusion, thermal and electrical noises induce nearly identical behaviors in the single-junction situation. For an optimal range of noise, the superparamagnetic tunnel junction is synchronized to the voltage drive.

III. NOISE-INDUCED SYNCHRONIZATION OF TWO ELECTRICALLY COUPLED JUNCTIONS

We now use our model to study the synchronization of coupled oscillators. We consider two identical junctions connected in series. The voltages V_1 and V_2 applied to each junction depend on the states of both junctions:

$$V_{1,2} = V_{ac}\frac{R_{1,2}}{R_1 + R_2}, \tag{12}$$

where $R_{1,2}$ are the respective resistances of the junctions. When the pinned layer of junction 1 is connected to the free layer of junction 2, the junctions are said to be head to tail. On the contrary, when the pinned layer of junction 1 is connected to the pinned layer of junction 2, the junctions are said to be head to head.

A. Thermal-noise-induced synchronization

In this section, we study the case where only thermal noise is involved. We consider two identical junctions whose electrical resistances are such that $R_{\mathrm{AP}} = 4R_P$, with R_{AP} (R_P) the resistance corresponding to the AP (P) state. The corresponding tunnel magnetoresistance is $\mathrm{TMR} = \frac{R_{\mathrm{AP}}-R_P}{R_P} = 300\%$. We apply a square periodic voltage of frequency $F_{ac} = 10$ kHz and amplitude $V_{ac} = 1.5$ V to the junctions.

1. Junctions connected head to tail

The numerical simulation is conducted in the same way as the single-junction study. A random number is generated for each junction. If both junctions have a random number lower than their switching probability, the precise times of switching corresponding to each random number are computed. Two cases arise. Either the times of switching are separated by less than 1 ns and both junctions switch simultaneously (1 ns is the typical duration of a switch [19]), or the times of switching are separated by more than 1 ns, in which case the junction with the lowest switching time switches first. Then the switching time of the other junction has to be recomputed because its switching probability is different now that the first junction has switched, modifying the applied voltage.

The frequencies of both junctions are plotted in black in Fig. 3. They are superimposed for all temperatures. The plateau at the frequency of the drive, characteristic of synchronization, is present between $T = 111$ and $T = 170$ K. Surprisingly, we observe the existence of a second plateau at half the frequency of the drive, between $T = 40$ and $T = 68$ K. Figure 4(A) present the evolution with time of the voltage drive and the resistances of both junctions. In Figs. 4(d)– 4(f), the temperature is 130 K, which corresponds to the plateau at the drive frequency. As expected, both junctions are locked in phase with the drive. In Figs. 4(a)– 4(c), the temperature is 60 K, which corresponds to the plateau at half the drive frequency. We observe that at each period of the drive, one junction is locked in phase with the drive while the other is blocked in the P state. The phase-locked junction alternates randomly from period to period.

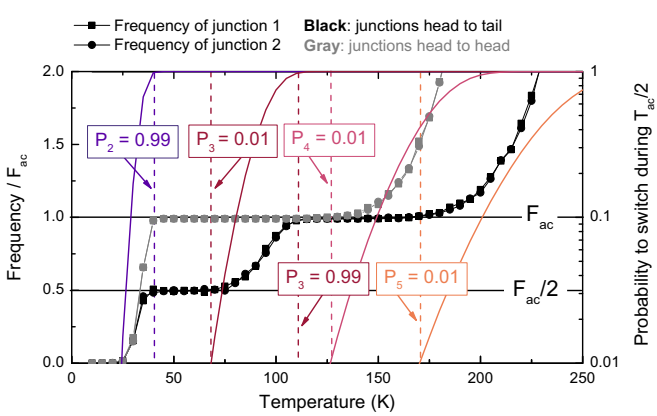

FIG. 3. The frequency of junctions is plotted vs temperature. The frequency of junction 1 (2) is represented with squares (circles). In the case where both junctions are head to tail (head to head), the symbols are black (gray). The drive frequency F_{ac} as well a half the drive frequency $\frac{F_{ac}}{2}$ are represented by black horizontal lines. The probabilities to switch during $\frac{T_{ac}}{2}$, P_2, P_3, P_4, and P_5 are represented by solid lines of color, from purple to orange. The dashed vertical lines represent the temperatures at which $P_2 = 0.99$, $P_3 = 0.01$, $P_3 = 0.99$, $P_4 = 0.01$, and $P_5 = 0.01$.

In the Appendix, we use further numerical simulations and our analytical model to investigate the influence of the tunnel magnetoresistance and the drive frequency on the existence and width of the plateaus. We observe that a high tunnel magnetoresistance widens the plateau at $F_{ac}/2$ and narrows the plateau at F_{ac}. A 300% tunnel magnetoresistance (TMR) is a good illustration of the effect of the coupling while maintaining a realistic tunnel magnetoresistance. A drive frequency of $F_{ac} = 10$ kHz enables the system to exhibit two significant synchronization plateaus, at F_{ac} and $F_{ac}/2$.

To get a quantitative understanding of this phenomenon, we define six different probabilities which correspond to the possible switching probabilities of the junctions for the different drive and resistances configurations:

(i) $P_1 = P_{\mathrm{AP}\to P}(-\frac{4V}{5})$,
(ii) $P_2 = P_{\mathrm{AP}\to P}(-\frac{V}{2}) = P_{P\to\mathrm{AP}}(+\frac{V}{2})$,
(iii) $P_3 = P_{P\to\mathrm{AP}}(+\frac{V}{5})$,
(iv) $P_4 = P_{P\to\mathrm{AP}}(-\frac{V}{5})$,
(v) $P_5 = P_{\mathrm{AP}\to P}(+\frac{V}{2}) = P_{P\to\mathrm{AP}}(-\frac{V}{2})$,
(vi) $P_6 = P_{\mathrm{AP}\to P}(+\frac{4V}{5})$.

When both junctions are in the same state, a voltage $\frac{V_{ac}}{2}$ is applied to each. When they are in different states, $\frac{4V_{ac}}{5}$ is applied to the junction in the AP state while $\frac{V_{ac}}{5}$ is applied to the junction in the P state.

Therefore, P_1 and P_6 correspond to the switching probabilities of a junction in the AP state when the other junction is in the P state. P_3 and P_4 correspond to the switching probabilities of a junction in the P state when the other junction is in the AP state. P_2 and P_5 correspond to the switching probabilities when both junctions are in the same state, P or AP.

In Fig. 3, the frequencies of junctions 1 and 2 as well as the probabilities P_2, P_3, P_4, and P_5 are plotted versus temperature. The probabilities P_1 and P_6 do not appear on this graph as $P_1 \simeq 1$ and $P_6 < 0.01$ within the studied temperature range. Figure 4(B) illustrates the switching cycles of both junctions.

The plateau at half the drive frequency can be interpreted as follows and is depicted in Fig. 4(B). We use the following example as a starting point: the drive voltage is $+V = 1.5$ V and both junctions are in the P state. (A similar reasoning can be made for any other initial conditions.) Figure 3 shows that $P_2 > 0.99$. Therefore, both junctions have a high probability (P_2) to switch in the AP state in the following half period $\frac{T_{ac}}{2}$. One junction switches to the AP state, as depicted in Fig. 4(B). The switching probabilities are P_6 for the junction in the AP state and P_3 for the junction in the P state. As both probabilities P_6 and P_3 are below 0.01, both junctions remain in their state

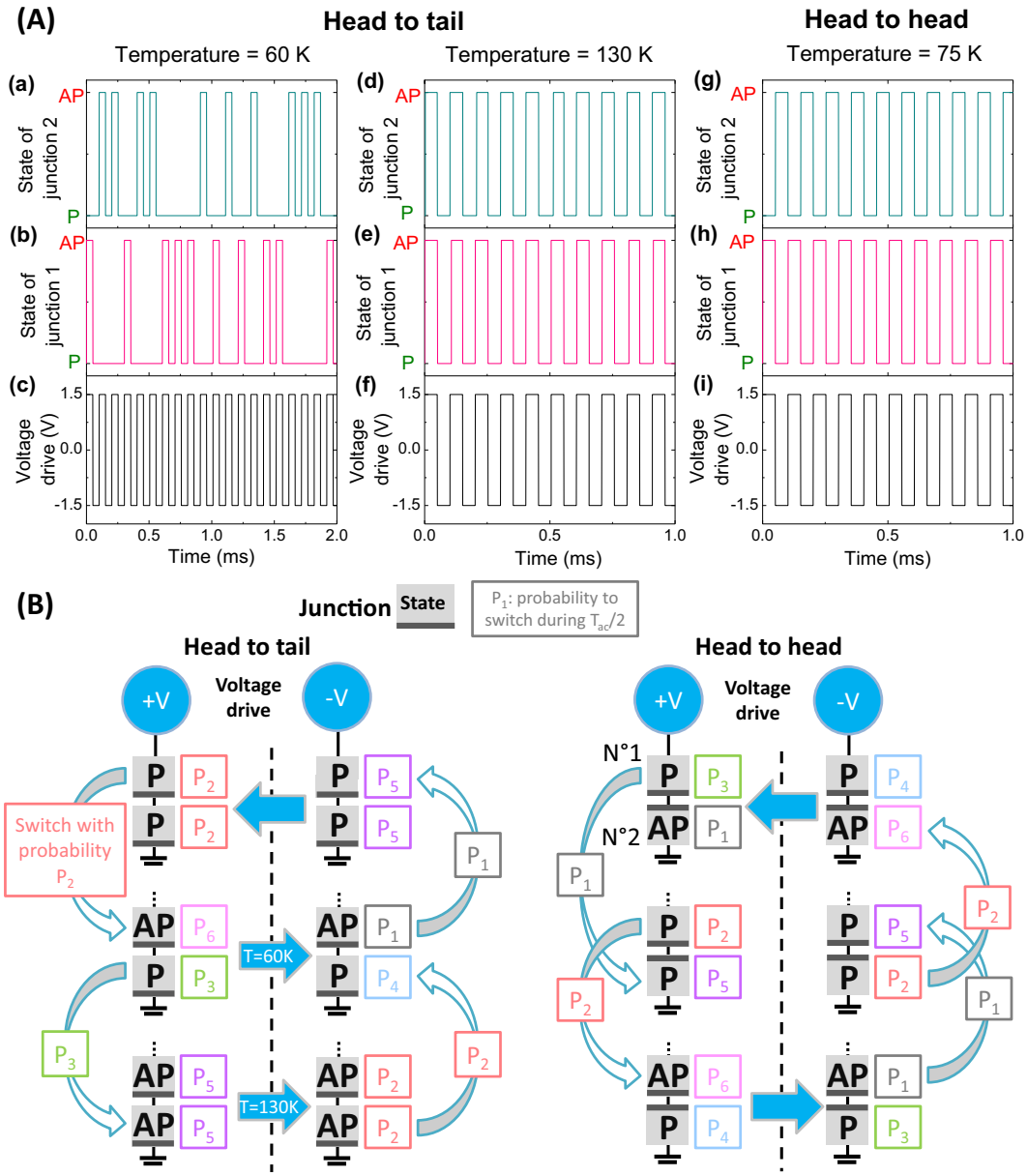

FIG. 4. (A): The temporal evolution—at a temperature of $T = 60$ K—of (a) the state of junction 2, (b) the state of junction 1, and (c) the amplitude of drive voltage V_{ac}, when the junctions are head to tail. The temporal evolution—at a temperature of $T = 130$ K—of (d) the state of junction 2, (e) the state of junction 1, and (f) the amplitude of drive voltage V_{ac}, when the junctions are head to tail. The temporal evolution—at a temperature of $T = 150$ K—of (g) the state of junction 2, (h) the state of junction 1, and (i) the amplitude of drive voltage V_{ac}, when the junctions are head to head. (B): Schematic depiction of the switching cycles that junctions 1 and 2 undergo. The gray rectangles represent the two junctions with their respective state (P or AP). For each configuration, the probability to switch during $\frac{T_{ac}}{2}$ is indicated on the left of each junction. Blue disks indicate the state of the drive voltage ($+V$ or $-V$). Blue horizontal arrows represent switches of the drive, while curved vertical arrows represent switches of the junctions. The probability of each switch is indicated on the arrow. When the junctions are head to head, the top junction is 1 and the bottom junction is 2.

until the next switch of the drive, depicted by the $T = 60$ K arrow in Fig. 4(B). When the drive switches from $+V$ to $-V$, the switching probabilities become P_1 for the junction in the AP state and P_4 for the junction in the P state. As $P_4 < 0.01$ while $P_1 > 0.99$, the junction in the AP state switches to the P state. Both junctions are in the P state with a switching probability of $P_5 < 0.01$: they remain in their state until the next switch of the drive. Then, their switching probabilities become P_2 and the cycle starts again. To summarize, at each oscillation cycle of the drive, one random junction is locked in phase with the drive while the other is blocked in the P state, leading to a mean frequency of $\frac{F_{ac}}{2}$ for both junctions. This is depicted in the Temperature =60 K panels of Fig. 4(A).

For $111 < T < 170$ K, P_3 is larger than 0.99. Considerations similar to the study of the 40–68 K range, depicted in Fig. 4(A), show that both junctions are locked in phase with the drive. This gives rise to the frequency plateau at F_{ac} and is illustrated in the Temperature =130 K panels of Fig. 4(A).

P_5 is the probability to phase unlock with the drive, when the drive is in both the $+V$ and $-V$ states Fig. 4(B). For temperatures above 170 K, P_5 is larger than 0.01, so glitches appear and synchronization is destroyed.

2. Junctions connected head to head

We now consider that junction 2 is connected head to head with junction 1. In that case, the voltage applied to the junction and governing the probabilities is $V_2 = -V_{ac}\frac{R_2}{R_1+R_2}$. We observe in Fig. 3(a) that the frequencies of junctions 1 and 2—plotted in gray—are equal at all temperatures. The frequency of the junctions increases with the temperature. Contrary to the case where the junctions are head to tail, a single plateau at the drive frequency F_{ac} is observed, between $T = 40$ and $T = 126$ K. Figures 4(g)–4(i) depict the evolution with time of the voltage drive, and the states of junctions 1 and 2, for a temperature of $T = 75$ K. This regime corresponds to the plateau and we observe that junction 1 is locked in phase with the drive, while junction 2 is locked in antiphase with the drive. These results can be interpreted with the same reasoning as in the head to tail case and as depicted in Fig. 4(B).

B. Electrical-noise-induced synchronization

In this section, we now control synchronization by injection of electrical noise. Contrary to the single-junction case, we show that in the two-junction case, electrical noise induces a behavior qualitatively different from the one induced by thermal noise. We consider two identical junctions with a tunnel magnetoresistance of TMR $= \frac{R_{AP}-R_P}{R_P} = 100\%$. As shown in the Appendix, this is high enough to have a signal that can be detected easily and low enough to exhibit a significant synchronization plateau. The switching probabilities are the averaged probabilities $\langle P_1\rangle$ to $\langle P_6\rangle$ over all possible values of $N(t)$.

In Fig. 5, the frequencies of junctions 1 and 2 as well as the average probabilities $\langle P_1\rangle$ to $\langle P_6\rangle$ are plotted versus the standard deviation of the noise distribution, both for the configurations where the junctions are head to tail and head to head.

1. Junctions connected head to tail

Both junctions have the same frequency at all levels of noise. We do not observe any synchronization at $\frac{F_{ac}}{2}$ for the junctions frequency in the range of noise for which $\langle P_2\rangle > 0.99$ and $\langle P_3\rangle < 0.01$. This can be interpreted as follows. In the thermal noise study, the escape rates are constant in time for a given temperature. The probability of switching at a given time is low but, because it is sustained over a long time, the probability for one junction to eventually switch is high. The situation is different when electrical noise is added on the drive. The distribution of the voltage from the electrical noise is Gaussian. As the noise is on the drive which is applied to both junctions, when a high-value voltage occurs, both junctions have a probability to switch that is close to one. Thus both junctions switch simultaneously. Therefore, when the drive switches to $+V$, either a high-value voltage event occurs and both junctions switch simultaneously in the AP state, or no high-value voltage event occurs and only one junction switches in the AP state while the other remains blocked in the P state, as explained in Sec. III A 1. As the noise

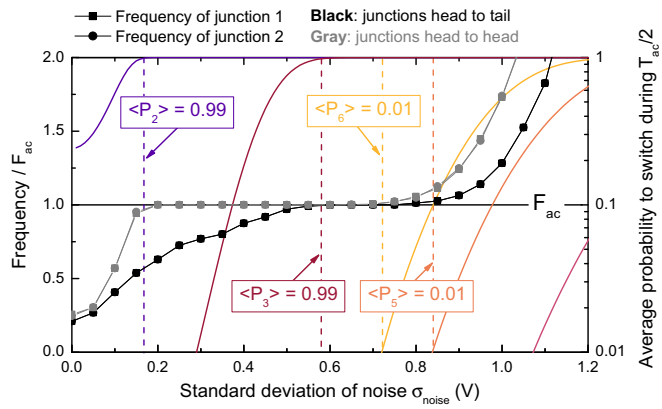

FIG. 5. The evolution of the frequency of the junctions is plotted vs the standard deviation of the Gaussian electrical noise. The frequency of junction 1 is represented with squares and the frequency of junction 2 is represented with circles. In the case where both junctions are head to tail, the symbols are black, whereas in the case where the junctions are head to head, the symbols are gray. The drive frequency F_{ac} as well as half the drive frequency $\frac{F_{ac}}{2}$ are represented by black horizontal lines. The average probabilities to switch during $\frac{T_{ac}}{2}$, P_1, P_2, P_3, P_4, P_5, and P_6 are represented by solid lines of color, from purple to light orange. The dashed vertical lines represent the electrical noise levels at which $P_2 = 0.99$, $P_3 = 0.99$, $P_5 = 0.01$, and $P_6 = 0.01$.

level is increased, more high-value voltage events occur and thus more simultaneous switches of the junctions occur. These observations pin a fundamental physical difference between internal and external noise.

For $0.58 < \sigma_{\text{noise}} < 0.84$ V, the frequency of the junctions is equal to the drive frequency F_{ac}. Indeed, $\langle P_3\rangle > 0.99$ and $\langle P_5\rangle < 0.01$. Both junctions are synchronized with the drive, in the same way as in the thermal noise study. For $\sigma_{\text{noise}} > 0.84$V, $\langle P_5\rangle$ is larger than 0.01, so glitches appear and synchronization is lost.

2. Junctions connected head to head

Both junctions have the same frequency for all levels of noise. For $0.16 < \sigma_{\text{noise}} < 0.72$ V, the frequency of the junctions is equal to the frequency of the drive F_{ac}. The behaviors of both junctions are the same as in the thermal noise study: junction 1 is locked in phase, while junction 2 is locked in antiphase with the drive. $\langle P_6\rangle > \langle P_4\rangle$, so synchronization is lost when $\langle P_6\rangle > 0.01$, which occurs when $\sigma_{\text{noise}} > 0.72$ V.

IV. CONCLUSION

In this work, we have investigated the noise-induced synchronization of one, and then two, electrically coupled stochastic magnetic oscillators with a periodic drive. We have shown that both thermal and electrical noise can induce synchronization of two coupled superparamagnetic tunnel junctions with a subthreshold voltage drive. When the junctions are head to tail, both are synchronized in phase with the drive for an optimal level of noise. When the junctions are head to head, one is synchronized in phase with the drive, while the other is synchronized in antiphase. Furthermore, this study has enabled us to highlight a fundamental difference between the

synchronization phenomena induced by thermal and electrical noise. Indeed, the fact that electrical noise makes the escape rates probabilistic themselves and that the electrical noise is correlated for both junctions lead to simultaneous switches of the two junctions—while this does not occur for thermal noise. We have provided an intuitive analytic understanding of how one or several coupled stochastic oscillators respond to a periodic drive.

This model will enable investigation of the interactions and synchronization of several stochastic oscillators in various configurations. The results will be useful for understanding and designing networks of coupled stochastic oscillators. Among potential applications of such networks, bioinspired computing is particularly promising, in particular as it allows taking advantage of noise and stochasticity for processing information. Indeed, networks of coupled oscillators can perform pattern recognition and classification through synchronization [20,21]. Toward that goal, noise level as well as drive frequency and amplitude provide handles to induce and suppress synchronization. Implementing these networks with subthreshold synchronization of superparamagnetic tunnel junctions would allow achieving such cognitive tasks at low energy cost.

ACKNOWLEDGMENTS

The authors acknowledge financial support from the FET-OPEN Bambi Project No. 618024 and the ANR MEMOS Grant No. ANR-14-CE26-0021. A.M. acknowledges financial support from the Ile-de-France regional government through the DIM Nano-K program. N.L. acknowledges financial support from the French National Research Agency (ANR) as part of the "Investissements d'Avenir" program (Labex NanoSaclay, Reference: ANR-10-LABX-0035).

APPENDIX: EFFECTS OF MAGNETORESISTANCE AND DRIVE FREQUENCY

In this Appendix, we study the effects of tunnel magnetoresistance and drive frequency on noise-induced synchronization of two superparamagnetic tunnel junctions, connected head to tail. Two identical superparamagnetic tunnel junctions of energy barrier such that $\Delta E = 30k_BT$ studied at $T = 50$ K are submitted to a periodic drive of amplitude $V = 1.5V_c$. The analytical model is used to compute the width in temperature of both synchronization plateaus, for various drive frequencies and magnetoresistance values. The results are presented in Fig. 6 for the $F = F_{ac}$ plateau and in Fig. 7 for the $F = F_{ac}/2$ plateau.

We observe that increasing the tunnel magnetoresistance widens the plateau at $F = F_{ac}/2$ and narrows the plateau at $F = F_{ac}$. When the junctions are in different states, the ratio between the voltage received by the junction in the AP state and the junction in the P state increases with the R_{AP}/R_P ratio, which strengthens the coupling and favors the $F = F_{ac}/2$ regime. For $R_{\mathrm{AP}} = R_P$, there is no tunnel magnetoresistance and the plateau at $F = F_{ac}/2$ is absent. The effect of drive frequency is nonmonotonous. Drive frequencies too high compared to the natural frequency of the junctions (which depends on the energy barrier) prevent the apparition of synchronization plateaus. On the other side, as temperature increases the frequency of the junction, lowering the drive

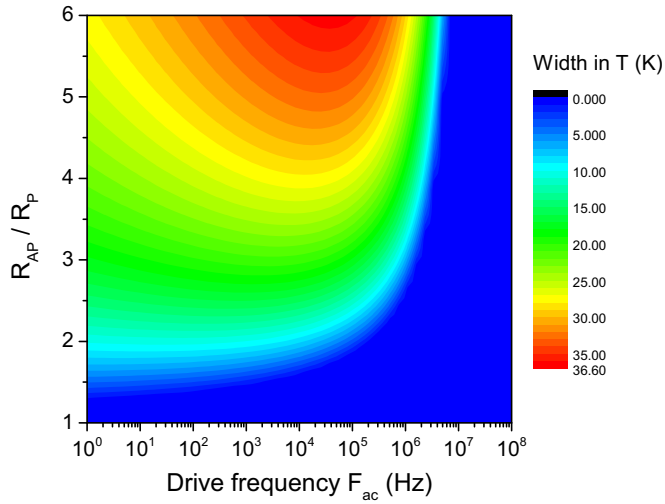

FIG. 7. Width in temperature of the synchronization plateau $F = F_{ac}/2$, as a function of the R_{AP}/R_P ratio and the drive frequency.

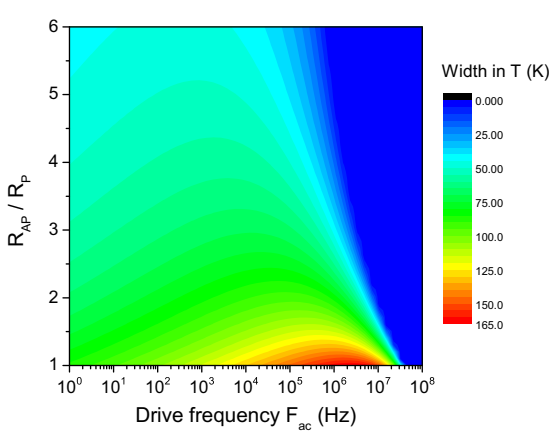

FIG. 6. Width in temperature of the synchronization plateau $F = F_{ac}$, as a function of the R_{AP}/R_P ratio and the drive frequency.

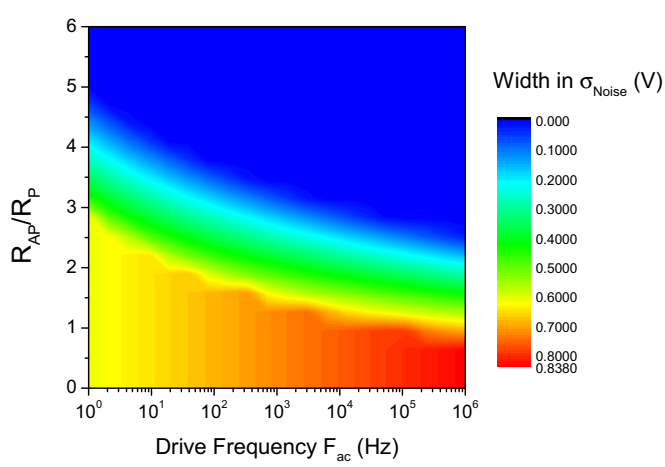

FIG. 8. Width in noise of the synchronization plateau $F = F_{ac}$, as a function of the R_{AP}/R_P ratio and the drive frequency.

frequency narrows the temperature range which can induce synchronization.

The same study is conducted in the case of synchronization induced by electrical noise. Figure 8 presents the influence of drive frequency and tunnel magnetoresistance on the width of the synchronization plateau at F_{ac}. We observe that the plateau is widest for low magnetoresistances and high drive frequencies. Numerical simulations show that no synchronization plateau can be observed at $F_{ac}/2$, regardless of the value of the magnetoresistance.

[1] W. Rippard, R. Heindl, M. Pufall, S. Russek, and A. Kos, Phys. Rev. B **84**, 064439 (2011).

[2] X. Cheng, C. T. Boone, J. Zhu, and I. N. Krivorotov, Phys. Rev. Lett. **105**, 047202 (2010).

[3] G. Finocchio, I. N. Krivorotov, X. Cheng, L. Torres, and B. Azzerboni, Phys. Rev. B **83**, 134402 (2011).

[4] M. d'Aquino, C. Serpico, R. Bonin, G. Bertotti, and I. D. Mayergoyz, Phys. Rev. B **84**, 214415 (2011).

[5] N. Locatelli, A. Mizrahi, A. Accioly, R. Matsumoto, A. Fukushima, H. Kubota, S. Yuasa, V. Cros, L. G. Pereira, D. Querlioz, J.-V. Kim, and J. Grollier, Phys. Rev. Appl. **2**, 034009 (2014).

[6] A. Mizrahi, N. Locatelli, R. Lebrun, V. Cros, A. Fukushima, H. Kubota, S. Yuasa, D. Querlioz, and J. Grollier, Sci. Rep. **6**, 30535 (2016).

[7] A. Neiman and L. Schimansky-Geier, Phys. Lett. A **197**, 379 (1995).

[8] J. F. Lindner, B. K. Meadows, W. L. Ditto, M. E. Inchiosa, and A. R. Bulsara, Phys. Rev. Lett. **75**, 3 (1995).

[9] F. Marchesoni, L. Gammaitoni, and A. R. Bulsara, Phys. Rev. Lett. **76**, 2609 (1996).

[10] M. Locher, D. Cigna, E. Hunt, G. Johnson, F. Marchesoni, L. Gammaitoni, M. Inchiosa, and A. Bulsara, Chaos: Interdisciplin. J. Nonlinear Sci. **8**, 604 (1998).

[11] A. Mizrahi, N. Locatelli, R. Matsumoto, A. Fukushima, H. Kubota, S. Yuasa, V. Cros, J.-V. Kim, J. Grollier, and D. Querlioz, IEEE Trans. Magn. **51**, 1 (2015).

[12] J. Slonczewski, J. Magn. Magn. Mater. **159**, L1 (1996).

[13] L. Berger, Phys. Rev. B **54**, 9353 (1996).

[14] W. F. Brown, Phys. Rev. **130**, 1677 (1963).

[15] J. C. Slonczewski, J. Magn. Magn. Mater. **195**, L261 (1999).

[16] Z. Li and S. Zhang, Phys. Rev. B **69**, 134416 (2004).

[17] A. Neiman, A. Silchenko, V. Anishchenko, and L. Schimansky-Geier, Phys. Rev. E **58**, 7118 (1998).

[18] J. A. Freund, L. Schimansky-Geier, and P. Hnggi, Chaos: Interdisciplin. J. Nonlinear Sci. **13**, 225 (2003).

[19] J. Sun, IBM J. Res. Dev. **50**, 81 (2006).

[20] F. C. Hoppensteadt and E. M. Izhikevich, Phys. Rev. Lett. **82**, 2983 (1999).

[21] T. Aonishi, Phys. Rev. E **58**, 4865 (1998).